

Cell Reports, Volume 40

Supplemental information

**STK25 inhibits PKA signaling
by phosphorylating PRKAR1A**

Xiaokan Zhang, Bryan Z. Wang, Michael Kim, Trevor R. Nash, Bohao Liu, Jenny Rao, Roberta Lock, Manuel Tamargo, Rajesh Kumar Soni, John Belov, Eric Li, Gordana Vunjak-Novakovic, and Barry Fine

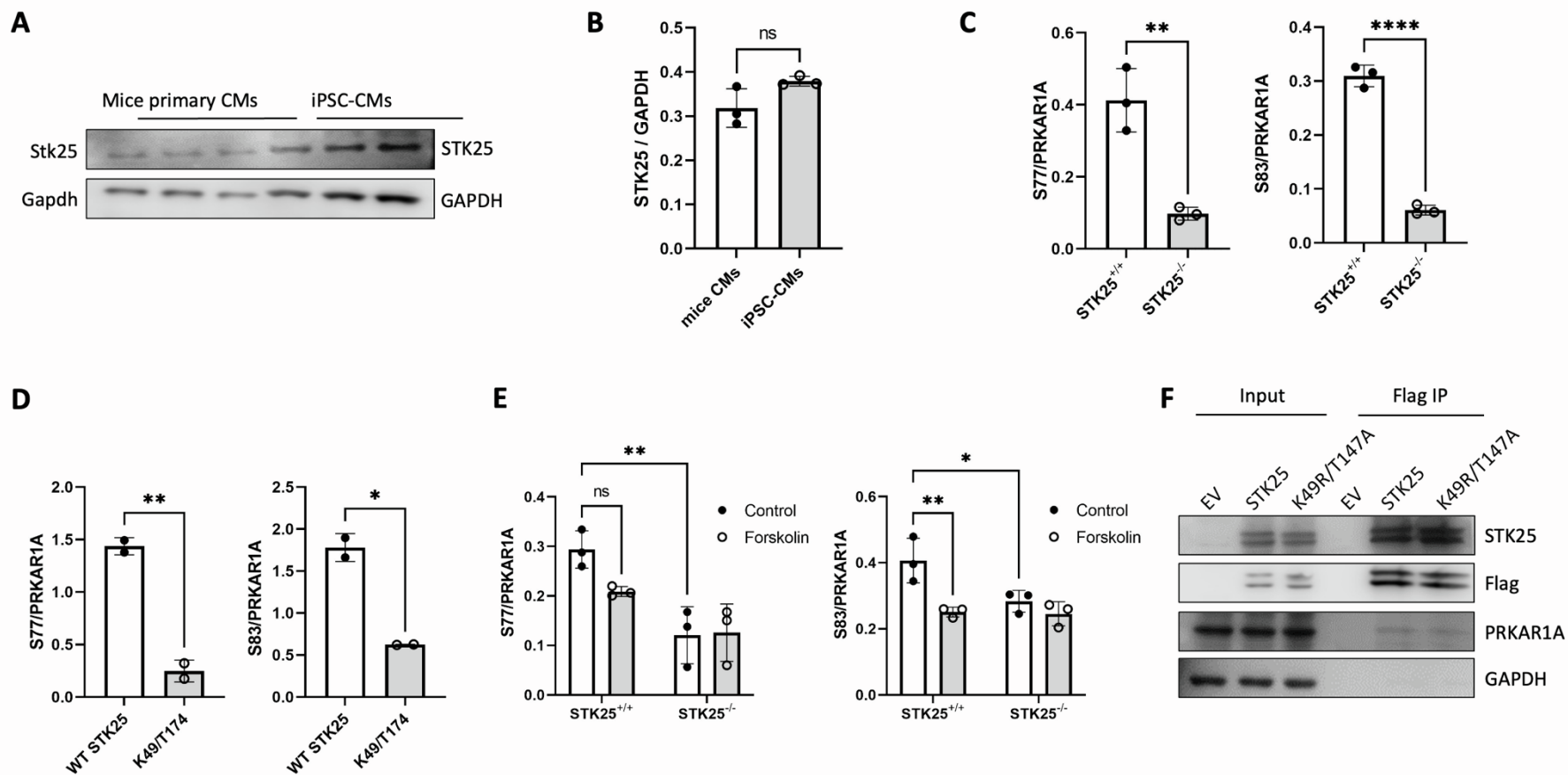


Figure S1. STK25 regulate PRKAR1A phosphorylation. Related to Figure 2. A) Immunoblot and B) densitometry of STK25 and GAPDH expression in primary cardiomyocytes isolated from adult mouse heart and in iPSC-CMs. C) Densitometry analysis of phospho-S77 and S83 relative to total PRKAR1A in immunoblot shown in Figure 2A. D) Densitometry analysis of phospho-S77 and S83 relative to total PRKAR1A in immunoblot shown in Figure 2B. E) Densitometry analysis of phospho-S77 and S83 relative to total PRKAR1A in immunoblot shown in Figure 2C. F) Co-immunoprecipitation experiments of either wild type or kinase dead (K49R/T147A) mutant of STK25 in HEK293T cells with overexpressed flag tagged STK25 protein and endogenous PRKAR1A. For all bar graphs in this figure, n=3 for each condition, Data presented as mean +/- SD, *p<0.05, **p<0.01, and ****p<0.0001 by student's t-test in S1B, S1C and S1D and two-way ANOVA with Tukey's adjustment for multiple comparisons in S1E.

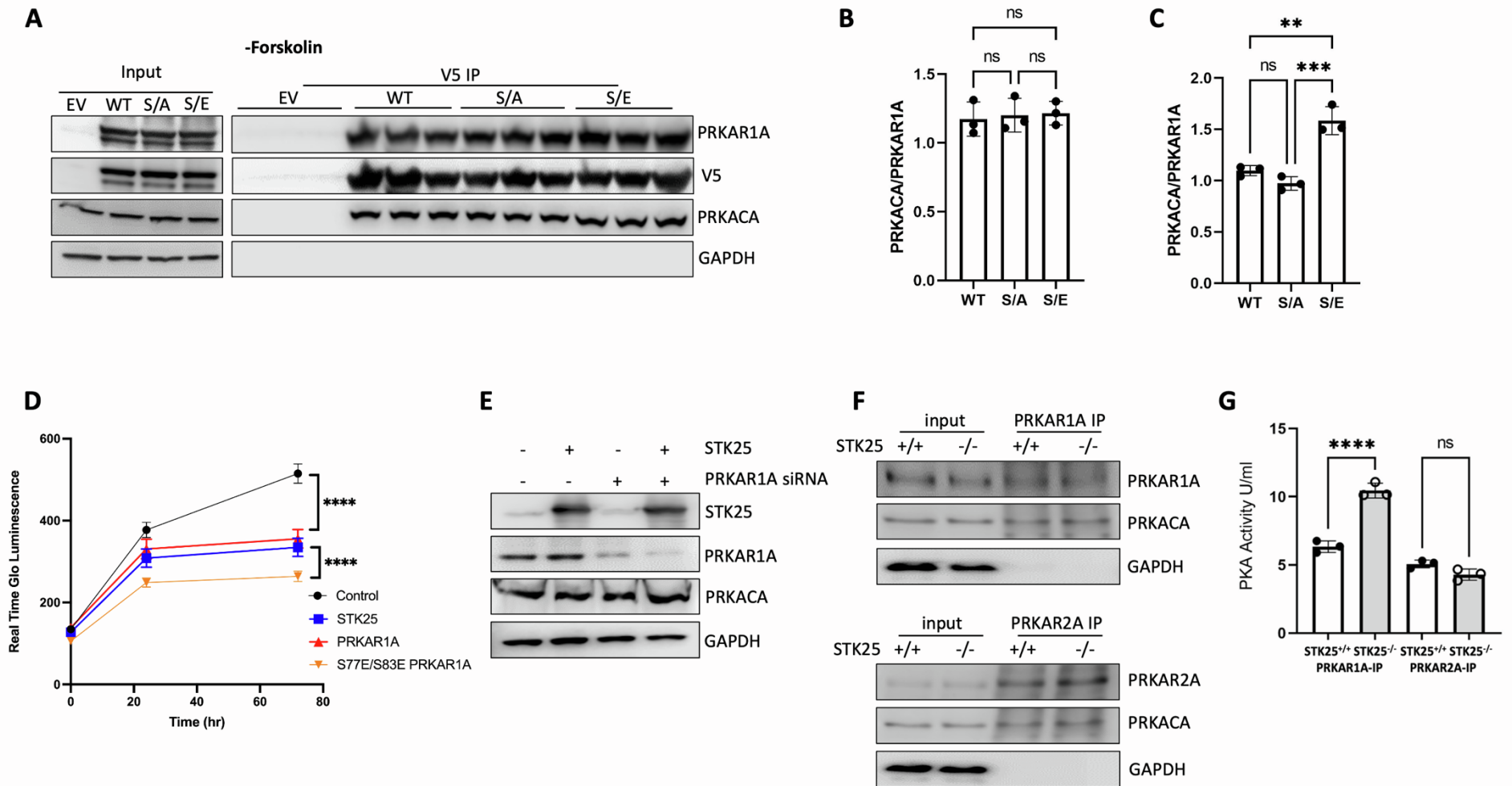


Figure S2. PRKAR1A phosphorylation regulates Type I PKA holoenzyme activity. Related to Figure 3. A) Co-immunoprecipitation of PRKAR1A-V5 with STK25 and PRKACA in HEK293T cells without forskolin treatment. B) Densitometry analysis of PRKACA relative to PRKAR1A in immunoblot shown in Figure S2A. $n=3$ for each condition. C) Densitometry analysis of PRKACA relative to PRKAR1A in immunoblot shown in Figure 3A. D) HEK293T cells transfected with the indicated vectors and assessed for growth by Real Time Glo (Promega) over three days. A representative Real Time Glo assay analyzed in sextuplicate \pm SEM is shown. E) Immunoblot demonstrating both overexpression of STK25 and knockdown of PRKAR1A in HEK293T cells shown in Figure 3D. F) Immunoprecipitations of PRKAR1A or PRKAR2A in STK25^{+/+} and STK25^{-/-} iPSC-CMs and immunoblotting for PRKAR1A or PRKAR2A, PRKACA and GAPDH. G) PKA activity of type I and II PKA holoenzymes precipitated from cell lysates of STK25^{+/+} and STK25^{-/-} iPSC-CMs ($n=3$ for each condition). For all graphs in this figure, data presented as mean \pm SD and analyzed in technical triplicates, ** $p<0.01$, *** $p<0.001$ and **** $p<0.0001$ one way ANOVA in S2B and S2C, two-way ANOVA with Tukey's adjustment for multiple comparisons in S2D, two-way ANOVA with Sidak's adjustment for multiple comparisons in S2G.

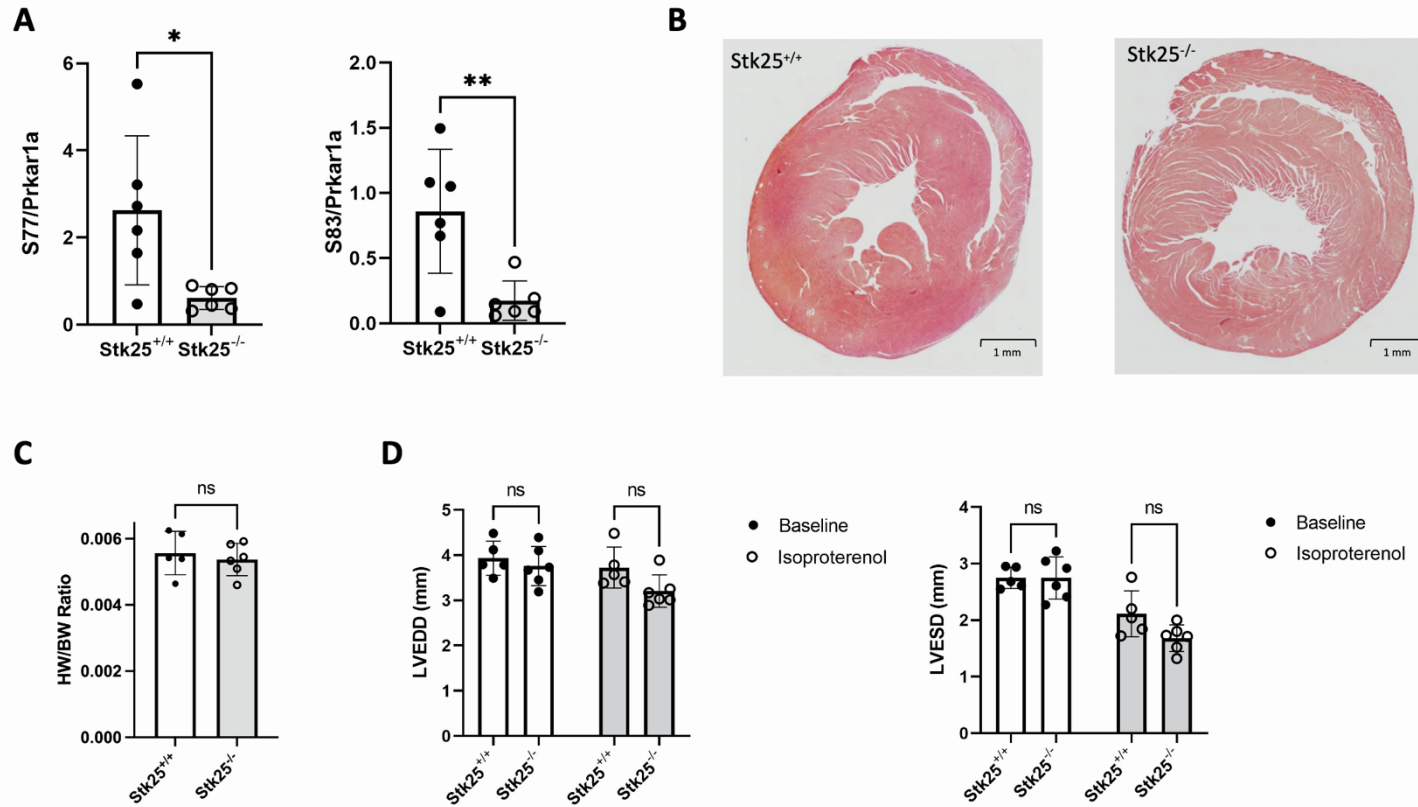


Figure S3. *Stk25* regulates PKA signaling in vivo. Related to Figure 4. A) Densitometry analysis phospho-S77 and S83 relative to total Prkar1a in immunoblot shown in Figure 4A. B). Representative pentachrome staining of mid ventricle sections of 20-week-old *Stk25*^{+/+} and *Stk25*^{-/-} mice. C) Heart weight (HW) to body weight (BW) ratio of mouse hearts at 20 weeks. D) Chamber measurements LVEDD (mm) and LVESD (mm) of mice at baseline and treated with isoproterenol. n=5 for *Stk25*^{+/+} and n=6 for *Stk25*^{-/-} mice. Data presented as mean +/- SD and analyzed in technical triplicates, statistical significance was tested with student's t-test in S3A, Welch's t-test in S3C, and repeated measures 2-way ANOVA with Sidak's correction for multiple comparisons in S3D.

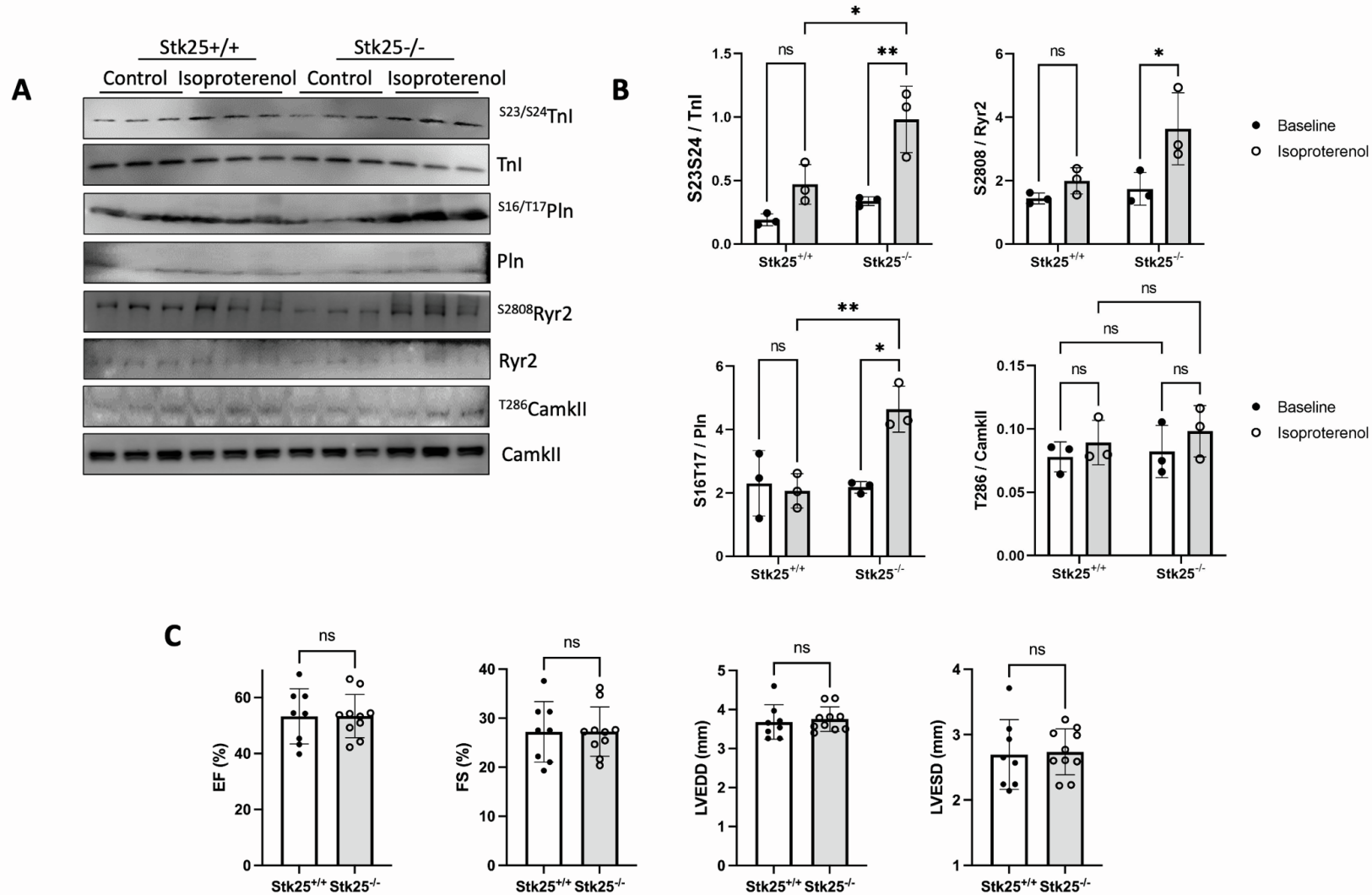


Figure S4. Stk25 knockout and beta-adrenergic response. Related to Figure 4. A) Immunoblot of phospho-S23/S24 and total Tnl, phospho-S16/T17 and total Pln, phospho-S2808 and total Ryr2, phospho-T286 and total CamkII in *Stk25^{+/+}* and *Stk25^{-/-}* whole heart lysates with and without isoproterenol injection. n=3 for each condition. B) Densitometry analysis of phospho-S23/S24 relative to total Tnl, phospho-S16/T17 relative to total Pln, phospho-S2808 relative to total Ryr2, phospho-T286 relative to total CamkII in immunoblot shown in Figure S4A, n=3 for each condition. C) Echocardiographic measurements of LV function and size in a survival cohort at 52 weeks for *Stk25^{+/+}* (n=8) and *Stk25^{-/-}* (n=10). Data presented as mean \pm SD, * p <0.05, ** p <0.01, statistical significance was tested with two-way ANOVA with Tukey's correction for multiple comparisons in S4B and Welch's t-test for S4C.

Patient Characteristics (n=17)		
	Age (SD)	49.47 (12.8)
	Gender (Male%)	82.4
	BMI (SD)	24.4 (3.3)
Cardiomyopathy		
	Non-ischemic (%)	70.6
	Ischemic (%)	29.4
Comorbidities		
	Hypertension (%)	17.6
	Hyperlipidemia (%)	29.4
	Diabetes(%)	23.5
Heart Function		
	Ejection Fraction (%)	17.9
	LVAD	88.23
	Inotrope	35.3
Medical Therapy		
	ACEi/ARB/ARNI	29.4
	Beta Blocker	76.5
	MRA	52.9
	Anticoagulation	88.23
	Antiarrhythmic	41.2

Table S1. Patient characteristics of end stage heart failure samples. Related to Figure 4.

Abbreviations: SD, standard deviation; BMI, body mass index; LVAD, left ventricular assist device; ACEi, angiotensin converting enzyme inhibitor; ARB, angiotensin II receptor blocker; ARNI angiotensin II receptor blocker and neprilysin inhibitor; MRA, mineralocorticoid receptor antagonist.